PROCEEDINGS, Fire and Evacuation Modeling Technical Conference (FEMTC) 2014
Gaithersburg, Maryland, September 8-10, 2014

SOOT DEPOSITION AND GRAVITATIONAL SETTLING MODELING AND THE IMPACT OF PARTICLE SIZE AND AGGLOMERATION

Floyd, J.[1], Overholt, K.[2], and Ezekoye, O.[3]

[1]Hughes Associates
3610 Commerce Dr. #817
Baltimore, MD, 21227 USA
e-mail: jfloyd@haifire.com
[2]Fire Research Division
National Institute of Standards and Technology
Gaithersburg, MD, 20899 USA
[3]Department of Mechanical Engineering
The University of Texas Austin
Austin, TX, 78712, USA

ABSTRACT

Soot concentrations are generally over predicted during the typical application of fire models. The addition of soot deposition and gravitational settling mechanisms to Fire Dynamics Simulator (FDS) results in improved predictions; however, those predictions are highly dependent upon assumptions of soot particle size. Large particle sizes appear to be needed to get FDS predictions on soot concentration to match measured data. Simple predictions of (and experimental data on) aerosol agglomeration show that compartment fires can result in significant amount of large particles sizes; however, the simple predictions do not fully account for the particle sizes needed to match the measured data. Recommendations on additional research and data collection are made to develop improved soot modeling capabilities.

NOMENCLATURE

B	particle mobility factor (s/kg)
Cn	Cunningham slip factor
D_B	Brownian diffusion constant (m^2/s)
Fu	Fuchs factor (m^2)
g	gravitational acceleration (m/s^2)
i,j,k	indices
k_B	Boltzmann constant (J/K)
Kn	Knudsen number
K_{th}	thermophoretic deposition constant
m	mass/particle size (kg)
N	number density (number/m^3)
r	radius (m)
R	removal term (number/m^3)
Re	Reynolds number
S	source term (number/m^3)
Sc	Schmidt number
t	time (s)
T	temperature (K)
u	velocity (m/s)
x	position (m), particle size (kg)

Greek

ε_S	sticking factor
ε_{PK}	collision efficiency
χ_d	shape factor
η	bin weighting factor
Φ	agglomeration kernel (m^3/number·s)
λ	mean free path (m)
μ	viscosity (kg/(m·s))
ν	kinematic viscosity (m^2/s)
ω	particle size (kg)
ρ	density (kg/m^3)
τ^+	dimensionless stopping distance

Subscripts

a	aerosol
dep	deposition
dt	diffusive-turbulent
g	gas, gravitational
th	thermophoretic
∞	ambient

INTRODUCTION

It has been previously reported [1] that while FDS easily predicts concentrations of major product species in well ventilated fires, that it has typically over predicted soot levels. This can be seen in Fig. 1 below which shows FDS predictions of carbon dioxide and soot densities vs. experiment in the NIST/NRC Benchmark Series 3 Test [2] (description provided later in the paper). As seen predictions of carbon dioxide generally lie within the experimental error (uncertainty of 13 %) and do not have a significant bias, but soot densities are greatly over predicted (experimental uncertainty of 30 %). One explanation for this would be the use of an incorrect soot yield in the input file; however, for this test series the soot yield was measured using the same burner as used in the test and the uncertainty in that measurement is only 20 %. It could be that the soot yield changed with the

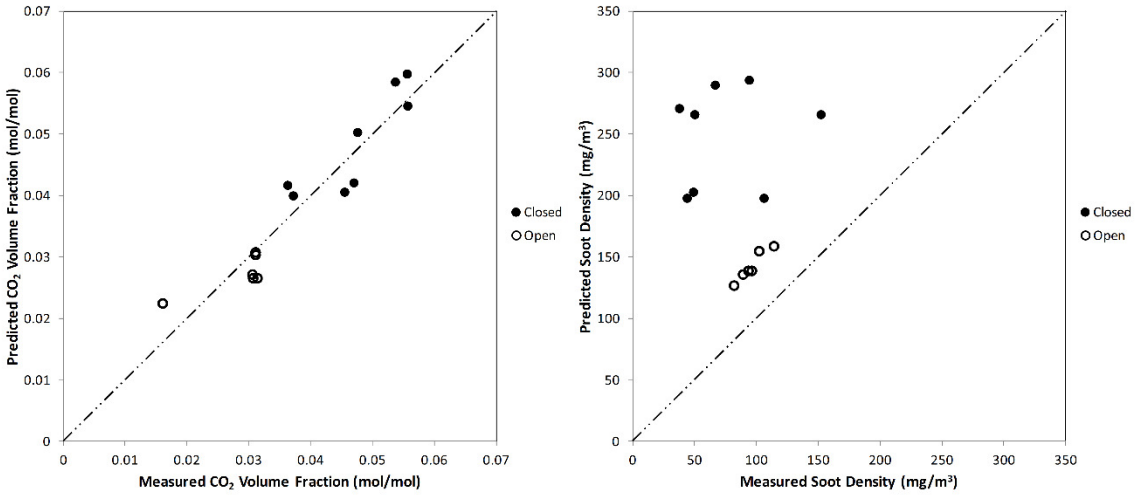

Figure 1: NIST/NRC Benchmark Series 3 CO2 concentration (left) and soot density (right) at end of steady burning without soot deposition. Filled circles indicate tests with the compartment closed door and unfilled with the door open.

This leaves removal of soot via deposition and gravitational settling. The Series 3 results suggest this is the case as FDS predictions are significantly better for the open door tests (where soot has less time to deposit or settle) then for closed door tests. Previous efforts [1] to model soot deposition using FDS v5 showed a significant improvement in predictions with the incorporation of some simple deposition mechanisms. This earlier work has been carried into the development of v6.

AEROSOL DEPOSITION

Traditionally, fire models have treated soot like a gas. An underlying assumption is that soot particles are sufficiently small that their terminal velocity is small compared to the ambient velocity. This assumption may not hold; however, for larger soot particles or in regions where the ambient velocities are low. There are a number of phenomena that cause deposition: thermophoresis (where temperature gradients push the aerosol towards or away from the surface), gravitational settling, diffusive deposition (where the aerosols move along the boundary layer concentration gradient), and turbulent deposition (essentially impact deposition due to a turbulent boundary layer). Other phenomena, such as electrical fields, can also result in deposition but are not considered in FDS due to their relatively small contribution in compartment fire scenarios [4].

Gravitational Settling

The gravitational settling velocity is given by [5]

$$u_g = g m_a \frac{\mathrm{Cn}}{6\pi\chi_d \mu r_a} \tag{1}$$

where m_a is the particle mass, χ_d is a shape factor, μ is the dynamic viscosity of air, r_a is the particle radius, and Cn is the Cunningham slip correction factor given by [6]

$$\mathrm{Cn} = 1 + 1.25\mathrm{Kn} + 0.41\mathrm{Kn}^{-0.88/\mathrm{Kn}} \tag{2}$$

where Kn is the particle Knudsen number given by the ratio of the mean free path of the gas to the particle radius. The mean free path of a gas is proportional to its temperature, thus Kn is computed as [7]

$$\mathrm{Kn} = \frac{\lambda}{r_a}\frac{T_g}{T_\infty} \tag{3}$$

where λ is the mean free path of gas molecules and is 0.065 μm at a temperature of 25 °C and atmospheric pressure.

For each aerosol species in the gas phase, a gravitational settling velocity is calculated and imposed on the convective term (in the z-direction) in the FDS species transport equation. This approach is similar to the drift flux model for smoke transport described in Hu et al. [8]. The gravitational settling velocity is also included in the total deposition velocity to deposit aerosols onto upward-facing flat surfaces, as described below.

Thermophoretic Deposition

The thermophoretic deposition velocity is computed as

$$u_{th} = \frac{K_{th}}{T_g}\frac{\mathrm{d}T}{\mathrm{d}x} \tag{4}$$

This requires the wall temperature gradient, which is only resolved in a DNS simulation. For an LES simulation, the temperature gradient is computed from the wall heat transfer coefficient. The deposition routine uses the same heat transfer coefficient, *h,* that is computed for wall heat transfer.

$$\frac{\mathrm{d}T}{\mathrm{d}x} = \frac{h\left(T_g - T_w\right)}{k_g} \tag{5}$$

K_{th} is the thermophoretic velocity coefficient and is calculated using the following correlation [9]

$$K_{th} = \frac{2C_s\left(\alpha + C_t \mathrm{Kn}\right)\mathrm{Cn}}{\left(1+3C_m \mathrm{Kn}\right)\left(1+2\alpha + C_t \mathrm{Kn}\right)} \tag{6}$$

where C_s=1.17 is the thermal slip coefficient, α is the ratio of the gas conductivity to the particle conductivity, C_m=1.14 is the momentum accommodation coefficient, and C_t=2.18 is the thermal accommodation coefficient.

Turbulent Deposition

The diffusion-turbulence deposition velocity depends upon the flow regime (diffusion, diffusion-impaction, or inertia-moderated). The deposition velocity for these regimes is given below [10].

$$u_{dt} = \begin{cases} 0.086\mathrm{Sc}^{-0.7} u_\tau & \tau^+ \le 0.2 \\ 3.5\times10^{-4}\tau^{+^2} u_\tau & 0.2 < \tau^+ \le 22.9 \\ 0.17 u_\tau & \tau^+ > 22.9 \end{cases} \tag{7}$$

where Sc is the particle Schmidt number, or the ratio of the kinematic viscosity to the Brownian diffusion coefficient of the particle (ν/D_B), u_τ is the wall friction velocity computed by the wall model, and $\tau+$ is the dimensionless stopping distance given by [11]

$$\tau^+ = \frac{\rho_a\left(2r_a\right)^2}{18\mu^2} u_t^2 \rho_g \tag{8}$$

Total Deposition

The total aerosol deposition velocity to surfaces, u_{dep}, is determined by assuming the deposition phenomena are independent, computing a deposition velocity for each mechanism, and then summing them. Note gravitational settling is only included at boundaries if the surface is upwards facing, otherwise, the gravitational component is handled by the species transport equation modification, this process is depicted in Fig 2. If the aerosol is located in a gas-phase cell adjacent to a wall, then the aerosol is removed from the gas-phase and deposited onto the wall surface by the amount calculated by

$$\Delta\rho_{a,dep} = \rho_a u_{dep} \frac{\Delta t}{\Delta x} \tag{9}$$

where $\Delta\rho_{a,dep}$ is the change in aerosol density due to deposition, ρ_a is the ambient density of the aerosol, Δt is the size of the time step, and Δx is the size of the grid cell. The accumulated aerosol density that deposits to surfaces, $m''_{a,dep}$, is tracked by calculating

$$m''_{a,dep,new} = m''_{a,dep,old} + \Delta\rho_{a,dep}\Delta x \tag{10}$$

at each time step. Finally, the amount of aerosol that deposits to a surface is removed from the gas-phase cell.

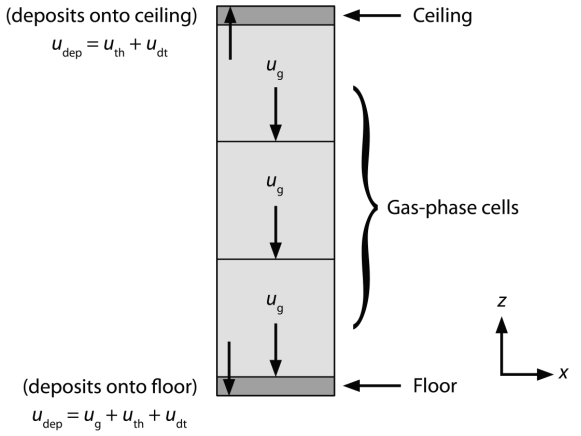

Figure 2: Implementation of soot deposition in FDS.

EFFECT OF SOOT SIZE ON DEPOSITION AND SETTLING

For each of the deposition and settling mechanisms, the inputs are the gas phase conditions plus the physical characteristics of the aerosols (primarily solid density and mean particle diameter). The density of the soot particles is taken as 1800 kg/m^3 [12]. Median aerodynamic diameters of soot particles can range from 0.05 μm for wood to 10 μm for acetylene, and a majority of fuels have median aerodynamic diameters less than 1 μm [13]. High-sooting fuels, such as toluene and acetylene, can produce large soot particle sizes (or "superaggregates") ranging from 10 μm to 100 μm [14,15]. Measurements of post-flame particle sizes from real world fuel sources (plastics, fabrics, etc.) [16] shows that most of the mass of soot, 70 % or more, is in small diameter particles (1 μm or less); however, there is measureable fraction, 5 % or more, of particles created at larger sizes (5 μm or more). The impact of particle size on deposition and settling was

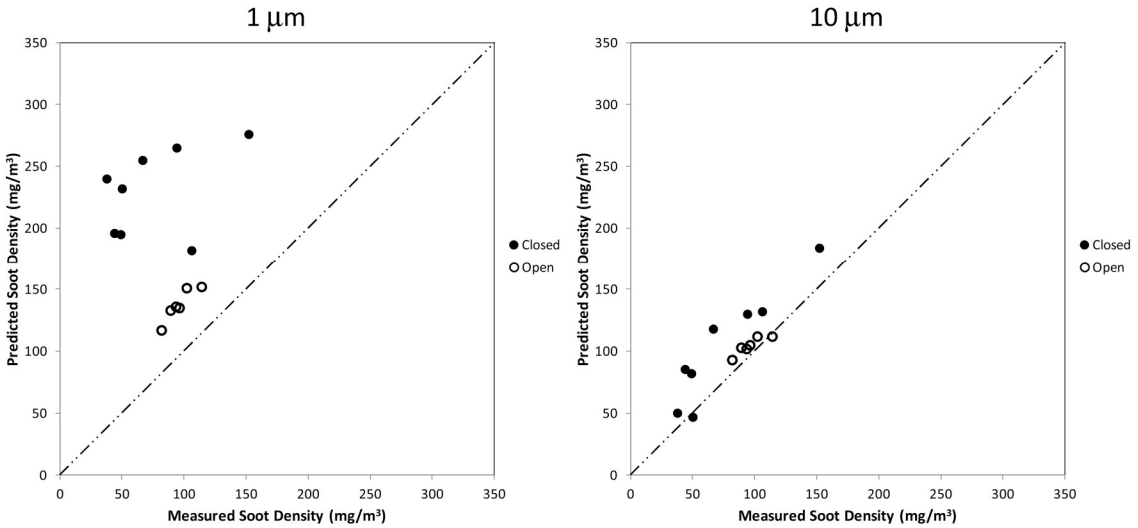

Figure 3: NIST/NRC Benchmark Series 3 soot density at end of steady burning assuming soot diameters of 1 µm (left) and 10 µm (right). Filled circles indicate tests with the compartment closed door and unfilled with the door open.

examined by simulating the Series 3 tests with either 1 µm or 10 µm soot particles. The results are shown in Fig. 3. As seen the assumption of 1 µm soot particles results in little change in the results without deposition shown in Fig. 1; however, the assumption of 10 µm soot particles results in a substantial improvement. At 10 µm gravitational settling (especially in the closed door cases) becomes a dominant mechanism (and likely explains the improvement by having soot settle below the measurement point which was high in the compartment). This raises a few questions. First, does the gravitational settling model reasonably predict the settling of soot? Second, for a polydisperse soot size distribution, how many sizes must be modeled? Lastly, can the need to have large particles to match the Series 3 test data be justified?

FM GLOBAL SETTLING CHAMBER

There is not a large body of data documenting the settling of soot particles with which to validate the settling algorithm discussed above. In one recent data set, FM Global performed a series of tests in which smoke from three plastic sources was injected into a 1 m^3 chamber and allowed to settle [17]. Smoke was created using a tube furnace and injected into the top of the chamber. A port at the bottom of the chamber was opened during injection to prevent pressurizing the chamber. Chamber temperatures remained close to ambient during the test. Measurements were made of the optical depth to obtain the mass of soot in the gas phase, and gravimetric measurements were made of the mass of soot settling on the floor of the chamber. Additionally, measurements were made of the particle size distribution over the length of the test. Size distribution measurements show that, following the smoke injection period, the size distribution did not change greatly over the length of the test. Results were presented as the fraction of smoke that deposited as a function of the mass of smoke present at the end of the injection period. Three simulations were made for the PVC deposition tests using a 3 cm grid resolution. Using the measured size distribution, these simulations divided the soot particles in 1, 3, or 6 size bins with each bin having an equal mass fraction and the bin characterized with its mass mean diameter. The respective results were 10 %, 62 %, and 68 % of the soot depositing on the lower surface of the chamber compared to approximately 45 % measured during the experiment. The results suggest that 3 size bins is reasonable for modeling the gravitational settling. Additionally, given the unknown uncertainties in the test data (size distribution errors and mass measurement errors), the 40 % error in the prediction of deposited mass is not unreasonable. For example a 10 % error in particle size would result in a 20 % error in settling velocity.

NIST/NRC SERIES 3 TEST SERIES

These experiments, sponsored by the US NRC and conducted at NIST, consisted of 15 large-scale experiments performed in June 2003. The fire sizes ranged from 350 kW to 2.2 MW in a compartment with dimensions 21.7 m by 7.1 m by 3.8 m high, designed to represent a compartment in a nuclear power plant containing power and control cables. The walls and ceiling were covered with two layers of marinate boards, each layer 0.0125 m thick. The floor was covered with one layer of gypsum board on top of a layer of plywood. The room had one door, 2 m by 2 m, and a mechanical air injection and extraction system. Ventilation conditions, the fire size, and fire

location were varied. Numerous measurements (approximately 350 per test) were made including gas and surface temperatures, heat fluxes and gas velocities. The burner heat release rate and species production rates were characterized under a hood prior to executing the compartment fire test matrix. While burning in a compartment is not the same as burning under a hood, the compartment fires were kept well ventilated (the fire was stopped if upper layer oxygen concentrations dropped below 15 %) and any reduction in ventilation efficiency for a compartment fire would be expected to increase the yield of soot and not decrease it. Therefore, it is deemed appropriate to use the hood measured data.

AGGLOMERATION

As seen in Fig. 3, matching the NIST/NRC Series 3 results at test end requires having large soot particles present; indicating that gravitational settling is an important mechanism in the long term. The previously referenced soot size measurements made by SP [16], however, do not show high mass fractions of large diameter particles. These measurements, however, were made promptly. In a compartment such as in the NIST/NRC Series 3, the soot can have a long residence time, as in the closed door tests where the residence time was up to 30 min. As time progresses, collisions between soot particles will lead to a reduction in the number density of particles and an increase in the particle size. This process is called agglomeration. Agglomeration of particles results from a number of mechanisms: Brownian agglomeration where the random walks of particles bring them into contact with one another, gravitational agglomeration where heavier particles fall onto smaller particles, and turbulent agglomeration where shear and inertia result in collisions between moving particles [4]. Agglomeration is governed by the following equation:

$$\frac{\partial N(m)}{\partial t} = \frac{1}{2}\int_0^m \Phi(\omega, m-\omega) N(\omega) N(m-\omega)\,\mathrm{d}\omega - N(m)\int_0^\infty \Phi(\omega, m) N(\omega)\,\mathrm{d}\omega - R(m) + S(m) \tag{11}$$

where Φ is an agglomeration kernel, $N(m)$ is the number density of particles of size m, R is a removal term (deposition, outflow, etc.), and S is a source term. The equation states that particles of size m are created by a source (e.g. the fire) or by colliding together two particles with sizes that sum to m, and that particles of size m are removed by colliding with either other particles or being lost due to deposition or outflow. The integrals in the above equation can be changed to summations by defining minimum and maximum particle masses and binning them into M bins as follows [18]:

$$s = \left(\frac{m_{\max}}{m_{\min}}\right)^{1/M}, \quad m_i = s m_{i-1}, \quad x_i = \frac{2m_i}{1+s} \tag{12}$$

where x_i is the mass assigned to the bin bounded by m_i and m_{i-1}. The integral agglomeration equation now becomes

$$\begin{aligned} \frac{\partial N_i}{\partial t} = & \sum_{j,k}^{j\geq k}\left(1-\frac{1}{2}\delta_{j,k}\right)\eta\Phi(j,k)N_j N_k \\ & - N_i\sum_{k=1}^{M}\Phi(j,k)N_k \\ & - R_i + S_i \end{aligned} \tag{13}$$

$$\eta = \begin{cases} \dfrac{x_{i+1}-m}{x_{i+1}-x_i} & x_i \leq m \leq x_{i+1} \\ \dfrac{m-x_i}{x_i - x_{i-1}} & x_{i-1} \leq m \leq x_i \end{cases}$$

where δ is the Kronecker delta function. The agglomeration kernel is given by the sum of Brownian (B), gravitational (G), shear (S), and inertial (I) agglomeration terms.

$$\Phi(m,\omega) = \frac{\Phi_B(m,\omega) + \Phi_G(m,\omega) + }{\sqrt{\Phi_S^2(m,\omega) + \Phi_I^2(m,\omega)}} \tag{14}$$

The Brownian agglomeration is given be the equation below where B is the particle mobility and Fu is the Fuchs factor.

$$\Phi_B(m,\omega) = \begin{matrix} 4\pi k_B T\left(B(m)+B(\omega)\right)\times \\ \left(r_m + r_\omega\right)\mathrm{Fu}(m,\omega) \end{matrix} \tag{15}$$

The particle mobility and the Fuchs factor are given by:

$$B(m) = \frac{\mathrm{Cn}}{6\pi\mu r_m} \tag{16}$$

$$\frac{1}{\mathrm{Fu}(m,\omega)} = \frac{1}{\mathrm{Fu}_1(m,\omega)} + \frac{1}{\mathrm{Fu}_2(m,\omega)};$$

$$\mathrm{Fu}_1(m,\omega) = \frac{\varepsilon_S \dfrac{r_m + r_\omega}{k_B T\left(B(m) + B(\omega)\right)} \times}{\sqrt{\dfrac{8k_B T}{\pi}\left(\dfrac{1}{m} - \dfrac{1}{\omega}\right)}} \qquad (17)$$

$$\mathrm{Fu}_2(m,\omega) = 1 + \frac{2\sqrt{\tilde{a}_m^2 + \tilde{a}_\omega}}{r_m + r_\omega}$$

Gravitational agglomeration is given by the equation below where ε_S is a sticking factor (assumed to be 1) and ε_{PK} a collision efficiency.

$$\Phi_G(m,\omega) = \frac{\varepsilon_S \varepsilon_{PK}(m,\omega)\left(r_m + r_\omega\right)^2 \times}{\left|u_g(m) + u_g(\omega)\right|} \qquad (18)$$

$$\varepsilon_{PK} = \frac{\min^2\left(r_m, r_\omega\right)}{2\left(r_m^2 + r_\omega^2\right)} \qquad (18)$$

Shear agglomeration and inertial agglomeration are given by the equations below.

$$\Phi_S(m,\omega) = \frac{\varepsilon_S \varepsilon_{PK}(m,\omega)\left(r_m + r_\omega\right)^3 \times}{\sqrt{\dfrac{8\rho\pi}{15\mu}\dfrac{0.03146 v^2}{d\,\mathrm{Re}^{3/8}}}} \qquad (19)$$

$$\Phi_I(m,\omega) = \frac{\varepsilon_S \varepsilon_{PK}(m,\omega)\left(r_m + r_\omega\right)^2 \times}{\left(\dfrac{512\rho\pi^3}{15\mu}\left(\dfrac{0.03146 v^2}{2r\,\mathrm{Re}^{3/8}}\right)^3\right)^{1/4} \times \dfrac{\left|u_g(m) - u_g(\omega)\right|}{g}} \qquad (20)$$

A Fortran program was written to perform an agglomeration calculation for a lumped volume. A range of particle diameters from 0.01 to 100 μm was considered, and the distribution of particle sizes in this range will be described later. The agglomeration kernel from VICTORIA [4], a US Nuclear Regulatory Commission code for estimating radionuclide emissions from severe accidents, was used. More information on the numerical details of the VICTORIA agglomeration kernel can be found in [4], which is freely available for download from Sandia National Laboratories. This Fortran program was used to perform agglomeration calculations for the Series 3 tests. The inputs to the program are the bin definitions, a time dependent soot production rate for each of the bins, the size of the lumped volume, and a volumetric loss rate to account for ventilation (i.e. the fraction of soot that is lost and replaced by ambient air). The program integrates Eq. 13 using a 1 s time step.

The soot source term was defined by first determining the mass production rate of soot using the reported heat release rate and measured soot yield. A soot particle size distribution was calculated by assuming the soot size distribution followed that for polyethylene reported in [16]. The measured size distribution from [16] was represented as a PDF that contained 150 bins (i.e., the value in each bin represents the fraction of soot produced in that bin). The soot source term consisted of the test time dependent mass production rate multiplied by the bin weighting factors. For a closed compartment test, the volume was assumed to be the entire compartment, and for an open compartment test, the volume was assumed to be that of the upper layer as reported in the test report. Where appropriate, a loss term was defined to represent the air exchange rate for either the open door or the mechanical HVAC system present for some of the tests. Removal by deposition and settling was ignored for this simple calculation. This was done for tests 1, 2, 3, 4, 5, 13, and 16, which represent all unique heptane tests (other heptane tests were replicates).

The results of the detailed agglomeration calculations were processed to collapse the 150 bins into three bins with diameters of 1, 3.16, and 10 μm (3.16 is the log mean of 1 and 10) for an open door test and for a closed door test. Figure 4 shows the results over time for Test 2 (closed door) and Test 3 (open door). Within 10 minutes, the open door test, Test 3 reaches a steady state size distribution that lasts until the fire ends (and the source term goes away). While 80 % of the source particles are created in the 1 μm bin, only 60 % of the particles remain in that bin during the test. In Test 2 the average particle size continuously increases as particles continue to agglomerate. By the end of the fire at ten minutes, only a quarter of the particles remain in the 1 μm bin, and a third of the particles are now in the 10 μm bin.

The results of the agglomeration program were used to define 3-bin particle size distributions for all of the Series 3 heptane tests. The 3-bin particle size distributions used for the FDS simulations were determined by averaging the 3-bin data shown in Fig. 4 over the steady-state fire portion of each test. For the data shown in Test 3 this resulted in bin weighting factors of 0.64, 0.27, and 0.09 respectively for the 1, 3.6, and 10 μm particle sizes. The FDS input files were modified to use three soot species with diameters

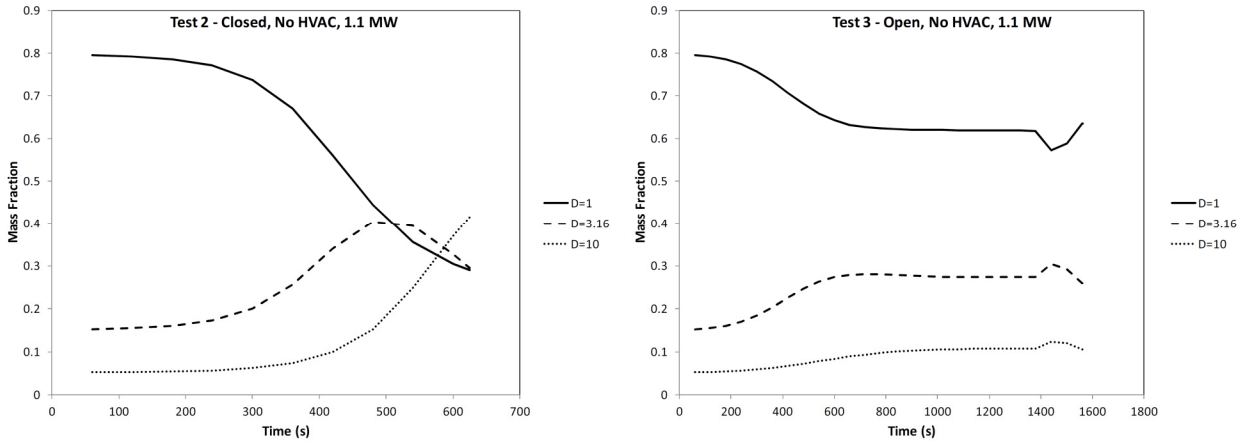

Figure 4: Result of agglomeration calculations for NIST/NRC Benchmark Series 3 Test 2 (left) and Test 3 (right).

of 1, 3.16, and 10 μm. The heptane reaction input was modified to produce the same soot yield, but with the soot mass allocated to the size bins based upon the results of the agglomeration calculation. The results of the FDS simulations with the post agglomeration size distribution are shown in Fig. 5. As seen there is a slight improvement over the 1 μm soot size results, but the results do not agree as well as the 10 μm size results.

The experimental error for the light extinction is estimated as a 9 % standard deviation based on component errors of the assumed mass extinction coefficient, voltage fluctuations in the measurement device, and errors in measuring the path length. Additional sources of error are the test heat release rate (5 % standard deviation) and the soot yield (11 % standard deviation). Combining these uncertainties results in an estimated uncertainty of the test soot measurement of a 15 % standard deviation (i.e. a 30 % expanded uncertainty). Utilizing the procedure from the FDS Validation Guide [19], the model error and bias are computed for each set of simulations, shown in Table 1. The table echoes the graphs in analytic form. The worst predictions are the assumption of no surface deposition followed by the assumption of 1 μm particles (7 % reduction in error and bias from no deposition), a three bin size distribution based on a simple agglomeration mode (17 % reduction), and the assumption of 10 μm particles (40 % reduction). The last, while biased high, still has an error that is about twice that of the experiment.

Table 1: Model error and bias for deposition simulations.

Simulation	Error	Bias
No Deposition	0.60	3.1
1 μm particles	0.56	2.9
3-bin, post agglomeration particles	0.50	2.6
10 μm particles	0.35	1.4

SUMMARY

Modeling the NIST/NRC Series 3 tests using the typical fire modeling approach of only treating soot as a gas results in significant over predictions of soot concentrations. Consideration of the FDS predictions for other quantities, the conditions that occurred during the tests, and the manner in which the fuel was characterized suggests that the issue is with the assumption of purely treating soot as a gas. Modeling soot as a gas that contains particles that are capable of agglomerating, settling, and depositing results in improved predictions in the soot concentration. Relatively large soot diameters are required to obtain predictions close the measured conditions, but these larger soot particle diameters are within the range of soot diameters that have been observed in various experiments, as described previously.

Predictions of soot deposition using the FM Global settling chamber indicate that one need not model a large number of particle sizes to obtain reasonable soot deposition predictions, as only slight changes were seen in going from three particle size bins to six particle size bins.

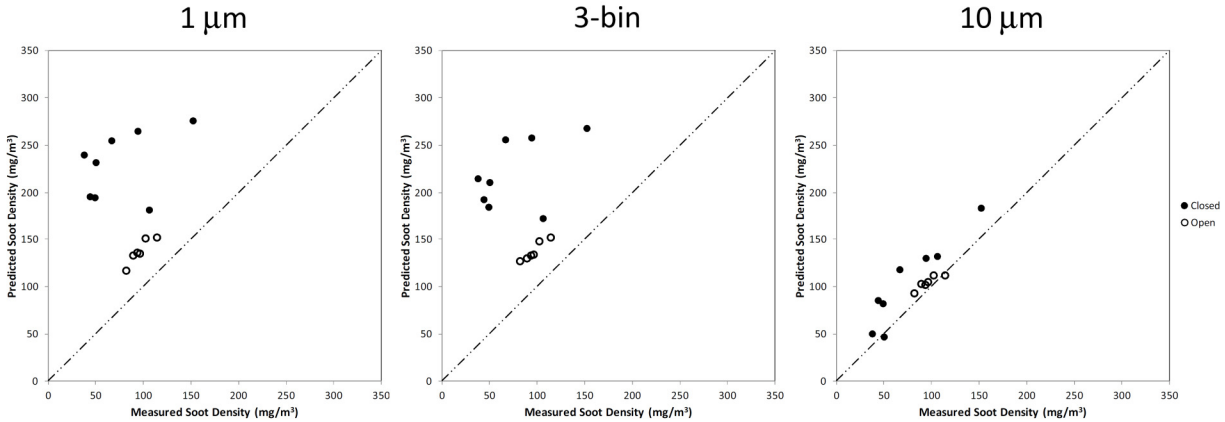

Figure 5: NIST/NRC Benchmark Series 3 for 1 µm particles (left), 3 particle size bins and post-agglomeration size distribution (middle), and 10 µm particles (right). Filled circles indicate tests with the compartment closed door and unfilled with the door open.

Post-flame soot size measurements show that the vast majority of soot particles are initially generated with fairly small diameters (under 1 µm). Predictions of the NIST/NRC Series 3 with 1 µm particle sizes and deposition and gravitational settling showed little improvement over FDS results without including these behaviors. However, these small particle sizes will not persist over time. Over time, soot particles will agglomerate and increase in size. Using the agglomeration kernel from VICTORIA, a simple agglomeration calculation for the NIST/NRC Series 3 tests results in an increase in the largest particles (10 µm or larger) from 5 % to 10 % of the overall particle mass for open door tests and from 5 % to over 30 % for closed door tests. Accounting for this size distribution in the deposition calculation results in 10 % improvement in the bias and error over that for just 1 µm particles. This performance, however, is still significantly worse than assuming the particles are all 10 µm particles. While agglomeration, gravitational settling, and deposition are part of the reason for the error between FDS predictions and the measured data, these phenomena do not explain all of the discrepancy.

There are other factors which might contributing to the prediction error that were not considered in this analysis.

- The agglomeration calculation is likely under predicting agglomeration due to its assumption of uniform soot concentrations over the entire compartment. The fire plume and ceiling jet regions of the flow will have significantly larger soot number densities than those seen once the soot mixes into the compartment. Agglomeration rates are proportional to the square of the number density; therefore, increases in number density will rapidly increase agglomeration rates in those regions of the flow.
- The bins used in the FDS simulations represented the average particle size over the NIST test. For the open doors this represents the particles present over much of the test. For the closed door tests, this biases the distribution towards the smaller particles present at the beginning of the test and will likely greatly underestimate the settling that occurred late in the closed door tests. That is had an agglomeration model been coupled to FDS a much better improvement would be expected.
- The experimentally measured values in the NIST/NRC Series 3 tests were made by light extinction. The extinction coefficient used to derive the mass concentration resulted from post-flame measurements of extinction and soot mass [20] and its application relies in part on the assumption that the particle sizes are less than that of the light used to measure the extinction. For immediate post-flame soot, this is true; however, given enough agglomeration this will no longer be the case. While little work has directly assessed this impact, tests do show that agglomeration results in an increase in the extinction coefficient. That is the use of the 8.7 m^2/kg is likely to under-predict soot in environments with significant agglomeration.
- The initial particle size distribution was assumed using data for small scale fires. If the actual fire source had a larger initial size distribution, then the rate of creation of large diameter soot particles due to agglomeration would increase.
- Some soot will be re-entrained into the fire. If some of that soot undergoes oxidation, then the effective soot production rate will decrease from that measured under the hood. This is not expected to be a large contributor to the error.

CONCLUSIONS

Overall, the results of this effort demonstrate that predictions in soot concentration can be improved by accounting for the dynamic aerosol behavior of soot: deposition, settling, and agglomeration. The results also indicate a need for additional research and experiments as follows:

- Develop an understanding of the impact of particle size and size distribution on the mass extinction coefficient.
- Characterization of particle size distributions for fuels over a range of fire sizes including smoldering sources.
- Making simultaneous gravimetric measurements of soot in addition to light extinction measurements.
- Measurements of deposition during large scale fire tests.
- Measurements of agglomeration during large scale fire tests.
- Investigation of the addition of agglomeration mechanisms to FDS in addition to deposition mechanisms along with methods to reduce the associated computational burden.

ACKNOWLEDGEMENT

This paper was prepared using Federal funds under award 70NANB11H172 from the National Institute of Standards and Technology, U.S. Department of Commerce. The statements, findings, conclusions, and recommendations are those of the author(s) and do not necessarily reflect the views of NIST or the U.S. Department of Commerce.

REFERENCES

[1] Floyd, J. and McDermott, R., "Modeling Soot Deposition Using Large Eddy Simulation with a Mixture Fraction Based Framework," *Interflam 2010: Proceedings of the Twelfth International Conference*, Interscience, 2010, pp. 755–764.

[2] Hamins, A., Maranghides A., Johnsson, R., Donnelly, M., Yang, J., Mulholland, G., and Anleitner, R., "Report of Experimental Results for the International Fire Model Benchmarking and Validation Exercise #3," National Institute of Standards and Technology, Report NIST SP 1013-1, Gaithersburg, MD, 2005, 156 p.

[3] Higgins, K., Jung, H., Kittleson, D., Roberts, J., and Zachariah, M., (2002) Size-Selected Nanoparticle Chemistry: Kinetics of Soot Oxidation, J. Phys. Chem 106:96-103, http://dx.doi.org/10.1021/jp004466f

[4] Bixler, N., "VICTORIA 2.0: A Mechanistic Model for Radionuclide Behavior in a Nuclear Reactor Coolant System Under Severe Accident Conditions," U.S. Nuclear Regulatory Commission, NUREG/CR-6131, Rockville, MD, 285 p.

[5] Davies, C., *Aerosol Science*, Academic Press, London, 1966.

[6] Cunningham, E. (1910), On the Velocity of Steady Fall of Spherical Particles. Proc. Roy. Soc. A, 83:357, http://dx.doi.org/10.1098/rspa.1910.0024.

[7] Sippola, N. and Nazaroff, W., "Particle Deposition from Turbulent Flow: Review of Published Research and Its Applicability to Ventilation Ducts in Commercial Buildings," Lawrence Berkeley National Laboratory. LBNL Report 51432, Berkeley, California, 2002.

[8] Hu,. X., Wang, Z., Jia, F., Galea, E., and Patel, M., "Simulating Smoke Transport in Large Scale Enclosures Using a Multi-Particle-Size Model," *Fire Safety Science -- Proceedings of the Tenth International Symposium*, International Association for Fire Safety Science, 2000, pp. 655-668, http://dx.doi.org/10.3801/IAFSS.FSS.10-445

[9] Brock, J. (1962). On the Theory of Thermal Forces Acting on Aerosol Particles. J. Coll. Sci., 17:768–780, http://dx.doi.org/10.1016/0095-8522(62)90051-X.

[10] McCoy, D. and Hanratty, T. (1977). Rate of Deposition of Droplets in Annular Two-Phase Flow. Int. J. Multiphase Flow, 3:319–331, http://dx.doi.org/10.1016/0301-9322(77)90012-X.

[11] Ludwig, W., Brown, D., Lehtinen, K., Pyykönen, J. Enriquez, J., Jokiniemi, J., Gamble, R., "CFD Simulation on Aerosol Impaction and Deposition Analysis in a Passive Containment Condenser," *8th International Conference on Nuclear Engineering. American*, Society of Mechanical Engineers, 2000.

[12] Lautenberger, C., de Ris, J., Dembsey, N., Barnett, J., and Baum, H., (2005), A Simplified Model for Soot Formation and Oxidation in CFD Simulation of Non-Premixed Hydrocarbon Flames, Fire Safety Journal, 40:141-176, http://dx.doi.org/10.1016/j.firesaf.2004.10.002

[13] Butler, K. and Mulholland, G. (2004), Generation and Transport of Smoke Components, Fire Tech, 40(2):149-176, http://dx.doi.org/10.1023/B:FIRE.0000016841.07530.64

[14] Kearney, S. and Pierce, F. (2012), Evidence of soot superaggregates in a turbulent pool fire, Combustion and Flame, 159(10):3191–3198, http://dx.doi.org/10.1016/j.combustflame.2012.04.011

[15] Soresnsen, W. et al. (2003), Observations of Soot Superaggregates with a Fractal Dimension of 2.6 in Laminar Acetylene/Air Diffusion Flames, Langmuir, 19(18):7560-7563, http://dx.doi.org/10.1016/j.combustflame.2012.04.011.

[16] Hertzberg, T., Blomqvist, P., Dalene, M., and Skarping, G., Particles and Isocyanates from Fires, SP Sweedish National Testing and Research Institute, SP Report 2003:05, Borås, 2003.

[17] Newman, J., Su, P., and Yee, G., "Smoke Deposition Velocity in Industrial Fire Environments," *Fire Safety Science -- Proceedings of the Tenth International Symposium*, International Association for Fire Safety Science, 2000, pp. 655-668, http://dx.doi.org/10.3801/IAFSS.FSS.10-655

[18] Higgins, D. and Davidson, M., "An Isothermal Model of Agglomeration in a Flash Smelting Reaction Shaft," *Fifth International Conference on CFD in the Process Industries*, CSIRO, 2006.

[19] McGrattan, K., Hostikka, S., Floyd, J., and McDermott, R., "Fire Dynamics Simulator Technical Reference Guide Volume 3: Validation," National Institute of Standards and Technology, Report NIST SP 1018-5, Gaithersburg, MD, 2010, 298 p.

[20] Mulholland, G. and Croarkin, C. (2000). Specific Extinction Coefficient of Flame Generated Smoke, Fire and Materials, 24:227-230, http://dx.doi.org/10.1002/1099-1018(200009/10)24:5<227::AID-FAM742>3.0.CO;2-9 .